JAAS

PAPER

View Article Online
View Journal

Cite this: DOI: 10.1039/c8ja00067k

Combustion generated nanomaterials: online characterization *via* an ICP-MS based technique. Part II: resolving power for heterogeneous matrices†

D. Foppiano, [ac] M. Tarik, [*a] E. Gubler Müller[b] and C. Ludwig [*ac]

Among the available online techniques to characterize combustion generated nanomaterials, the recently developed RDD-SMPS-ICP-MS (rotating disc diluter-scanning mobility particle sizer-inductively coupled plasma-mass spectrometry) setup is here suggested, due to its ability to provide simultaneously size-resolved elemental and quantitative information with a high time resolution. The successful calibration strategy presented in Part I will be applied here. To assess the resolving power of the technique regarding the elemental composition, two different applications with complex heterogeneous matrixes were considered: a mixture of several metal chlorides particles generated by the reaction of metal oxides (PbO, CdO, CuO, ZnO) with $CaCl_2 \cdot 2H_2O$ and secondary formed ZnO nano-objects released during the combustion of impregnated wood. The latter, especially, allowed considering the effect of the heterogeneous nature of a realistic process gas sample, where several gas species are emitted. The results of these experiments showed the ability of the SMPS-ICPMS system to distinguish and quantify the single contribution of a specific element in the overall particle size distribution (PSD).

Received 2nd March 2018
Accepted 7th August 2018

DOI: 10.1039/c8ja00067k

rsc.li/jaas

1 Introduction

Quantification and characterization of nanomaterials are becoming crucial to determine their fate and concentration in environmental samples. The possibility of using inductively coupled plasma mass spectrometry (ICP-MS) for that purpose has so far been extensively exploited,[2] leading to its prevalent use in single particle mode for the determination for engineered nanoparticles (ENP) in levels of concentration close to part-per-trillion (ppt).[3] The detection of particles is performed by acquiring transient signals with millisecond dwell times or even microsecond for an improved resolution and working range.[4] Certainly, the possibility of acquiring multiple isotopes in a short time represents one of the main points of interest, in particular in the determination of mixed particle with core–shell structure. Multiple elements detection was shown thanks to an improved nebulization efficiency using a micro-droplet generator or by employing a modified ICP-MS, like the prototype of ICP time-of-flight spectrometer (ICP-TOF-MS) presented by Borovinskaya *et al.*[5–8] Some limitations arise for the presence of naturally-occuring-nano-materials or if the concentration of dissolved analytes lie above the (ppt) level, for which different fraction or separation techniques have been combined in the past (*e.g.* asymmetric flow field-flow fractionation, filtration, coupling with ion-exchange resin or cloud point extraction, capillary electrophoresis, *etc.*).[9–13] Although initially conceived for atmospheric chemistry and detection of aerosol particles, sp-ICP-MS is moving towards becoming the leading routine analysis for the characterization of metal-containing nanomaterials principally in aqueous dispersion,[14] with size detection limit estimated for more than 40 elements.[15]

Other online techniques normally employed in aerosol research for the analysis of nanoparticles are either specifically optimized for atmospheric metal detection in a very low concentration range,[16] or particularly focused on organic gaseous emissions employing soft ionization techniques like HR-AMS (high-resolution aerosol mass spectrometry) or HR-ToF-AMS (high-resolution time-of-flight aerosol mass spectrometry),[17] which can only be applied to non-refractory materials (with boiling points below 600 °C). The use of SP-AMS (soot-particle aerosol mass spectrometry) or SPI-ToF-AMS (single-photon ionization time-of-flight mass spectrometry) presents major advantages in case of combustion emissions, such as the possibility to follow the transformation of primary

[a]Bioenergy and Catalysis Laboratory (LBK), Energy and Environment Research Division (ENE), Paul Scherrer Institut (PSI), 5232 Villigen PSI, Switzerland. E-mail: debora.foppiano@psi.ch; mohamed.tarik@psi.ch; christian.ludwig@psi.ch

[b]Laboratory of Biomolecular Research (LBR), Biology and Chemistry Division (BIO), Paul Scherrer Institut (PSI), 5232 Villigen PSI, Switzerland

[c]Environmental Engineering Institute (IIE), School of Architecture, Civil and Environmental Engineering (ENAC), École polytechnique fédérale de Lausanne (EPFL), CH 1015 Lausanne, Switzerland

† Electronic supplementary information (ESI) available. See DOI: 10.1039/c8ja00067k

organic aerosol (POA) occurring into the atmosphere and its impact on cloud formation. Also, studying in detail the change in composition and concentration of primary and secondary volatile organic compounds (VOC) could help to assess improvements in stoves design.[18] SP-AMS allows characterizing with high time resolution also metallic compounds even when linked to refractory materials, *e.g.* black carbon (rBC), although some drop in sensitivity for trace metals occur if they are not contained in rBC-aerosol particles.[19] Nevertheless, for all these systems an extensive data treatment and availability of fragmentation tables and datasets are required.

For relatively high concentration ranges of the analytes of interest and complex heterogenous matrixes, such as combustion emission measurements, the use of an online method focused on metallic or metal oxides particles analysis is of particular interest, even more if it involves a faster data treatment. Alternatively, the RDD-SMPS-ICP-MS technique is hereby proposed as a robust online analytical tool having high ability to provide simultaneously size-resolved elemental and quantitative information with a good time resolution. This study presents two different applications assessing the resolving power of the RDD-SMPS-ICP-MS setup in the determination of nanomaterials. The main features of the technique were already described in Part I,[1] where the calibration strategy was explained.

Using the calibration concept previously described, two different applications are presented: first, during evaporation experiments from a complex mixture of different oxides and second, during combustion of ZnO impregnated waste wood.

2 Materials and methods

2.1 Instrumentation

The PSD and the chemical composition of the nanomaterials in the flue gas were acquired online and simultaneously using a special in-house developed setup SMPS-ICP-MS with a rotating disc diluter (RDD) as introduction system. The main features and the operating conditions of RDD-SMPS-ICP-MS were already described in Part I.[1] In this second part the aerosol sources, only, were varying between the different sets of experiments, as shown in Fig. 1. In the evaporation experiments and for the calibration of the setup, a TGA was the instrument of choice and the operating conditions were kept in line with the previous work.[1] The combustion experiments, instead, were conducted with a tubular furnace (Heraus, RE 1.1), whose experimental conditions were already described elsewhere.[20]

2.2 Materials

Beside Zn, the calibration of the setup RDD-SMPS-ICP-MS was performed also for Cd, using an anhydrous $CdCl_2$ powder (Fluka, reagent grade ≥99%, 20899, GA10523). The evaporation experiments included a mixture of several commercial powders: PbO (Fluka, reagent grade ≥99%, 15338, GA2053), CdO (Merck, reagent grade ≥99%, 2015.0100, 212 K14082415), CuO (Merck, reagent grade ≥99%, 1.02766.0100, TP995866930), ZnO (Merck, reagent grade ≥99%, 8849.0100203, K16151449) and $CaCl_2 \cdot 2H_2O$ (Merck, reagent grade ≥99%, 111TA106282). ZnO impregnated sawdust samples were used to perform the combustion experiments. An in-house prepared ZnO suspension (0.3 wt%) was used to impregnate the beech sawdust samples, with a final concentration of 1.5 wt% of Zn; further details about the process and characterization analysis were reported elsewhere.[20]

2.3 Experimental conditions

2.3.1 Calibration experiment with $CdCl_2$ powder. In order to quantify the ICP-MS signal of Cd and to calibrate the RDD-SMPS-ICP-MS system, evaporation experiments of $CdCl_2$ powder were performed using a TGA as an aerosol source. The total gas flow inside the TGA was set to 100 ml min^{-1} (reactive gas O_2: 46 ml min^{-1}; protective gas Ar: 54 ml min^{-1}). An alumina crucible with nearly 40 mg of $CdCl_2$ anhydrous powder was placed in the furnace. In order to identify the most suitable temperature range for our experiments, thermochemical calculations were performed with HSC software (Fig. S1 in ESI†). Consequently, the TGA program for the calibration experiment was set as follows: the temperature was maintained constant at

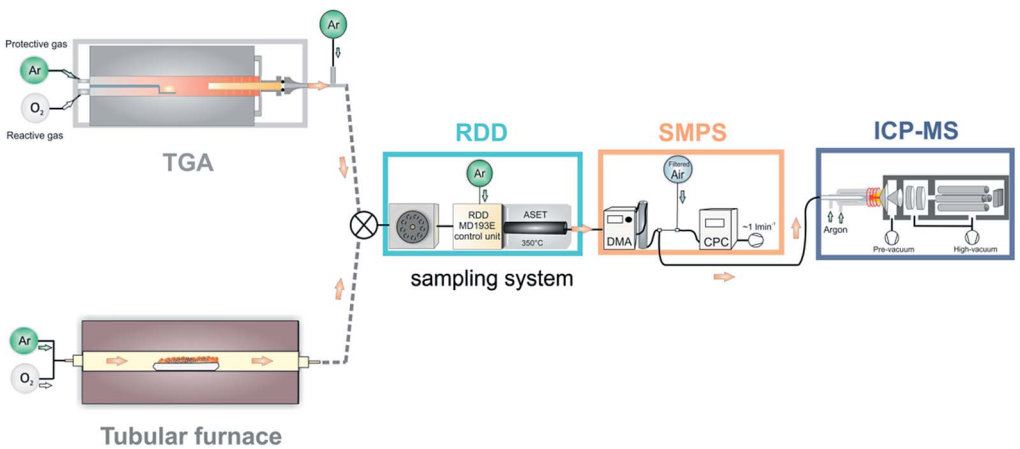

Fig. 1 Schematic of the setup RDD-SMPS-ICP-MS, including either a TGA or a tubular furnace as an aerosol source.

439°, 457°, 475°, 493° and 511 °C for 15 min each. The heating rate between these temperatures was set to 5 °C min^{-1} (Fig. S2 in ESI†). The isotope ^{111}Cd was measured by using ICP-MS with an integration time of 0.2 s (the general operating conditions of ICP-MS were already reported in Part I[1]).

2.3.2 Mixture of different metal chlorides particles analysis. PdO, CdO, CuO, ZnO, and $CaCl_2 \cdot 2H_2O$ powders were used as reactants to generate a mixture of different metal chlorides ($PbCl_2$, $CdCl_2$, $CuCl_2$ and $ZnCl_2$) particles. As a results of the thermochemical calculations with HSC software (Fig. S4 in ESI†), the temperature was increased between 25 °C and 850 °C at a constant heating rate of 10 °C min^{-1}, then an isothermal step at 850 °C was maintained for 20 minutes (Fig. S5 in ESI†), using O_2 as a reactive gas, in the same ratio reported above. A mixture of 25 mg of ZnO, 10 mg of PbO, 7 mg of CdO, 4 mg of CuO and 83 mg of $CaCl_2 \cdot 2H_2O$ was introduced into the furnace and the generated aerosol was initially diluted at the outlet of the TGA and in the RDD (total dilution factor: DF = 108) and later introduced into the DMA. Transient signals of the isotopes ^{206}Pb, ^{111}Cd, ^{63}Cu, and ^{66}Zn were acquired (with an integration time of 0.2 s each) by ICP-MS, while the CPC was measuring concurrently the particle concentration of the size-selected particles.

2.3.3 ZnO impregnated sawdust combustion. The combustion experiments on 400 mg of ZnO impregnated sawdust were conducted in a tubular furnace. The temperature program of 24 minutes was including a drying step, a fast pyrolysis from 300 to 900 °C, combustion at 900 °C and a fast after burning between 900 °C and 400 °C. The analysis by RDD-SMPS-ICP-MS was recorded only during combustion and afterburning. Further details can be found in a previous publication.[20]

3 Results and discussion

3.1 Mixture of different metal chlorides particles analysis

To assess the resolution power of the technique, a complex mixture of several metal chlorides particles generated by the reaction of metal oxides (PbO, CdO, CuO, ZnO) with $CaCl_2 \cdot 2H_2O$ was considered. The first purpose of these experiments was to distinguish the single contribution of each element in the overall particle size distribution (PSD). Although SMPS is performing the size-selection and providing information about the particle size, the volume-related concentration obtained (Fig. 2A) refers only to the overall amount of particles generated during the process. As a result of the time synchronization between the two instruments, the ICP-MS intensities can be also expressed as a function of particle size and, therefore, it is possible to determine the single-element contribution to the overall PSD. For instance, as can be seen in Fig. 2B, the signal relative to ^{206}Pb resembles quite closely the PSD measured in SMPS and results in a much higher intensity compared to all the other elements, *i.e.* the emission of particles containing Pb cover all PSD measured by SMPS. Furthermore, ^{111}Cd and ^{66}Zn follow the same emission pattern as Pb, even though the related intensity is lower. In the case of ^{63}Cu, instead, the evaporation occurred later on at a higher temperature, with a consistent contribution to the PSD only in the fraction of larger particles above 150 nm. In order to confirm the SMPS assumptions on spherical geometry, TEM (transmission electron microscopy) was employed to determine the particle morphology. Fig. S6 in ESI† shows an example of TEM micrograph; the metallic-chloride particles were sampled during another replicate operated in the same conditions like the experiment in Fig. 2.

The second purpose of these experiments regarded the quantification of metals content emitted over time.

Firstly, it was calculated that 272 μg min^{-1} (RSD% = 0.7) of the initial sample was released over time with a total loss of 17.1009 ± 0.0017 mg during the overall analysis, as can be seen in Fig. S7 in ESI.† Secondly, the contribution of two of the metals in the overall PSD was determined. In ref. 1 it was already shown how the ^{66}Zn ICP-MS signal could be quantified and expressed in ng cm^{-3}, thanks to the calibration strategy by coupling ICP-MS with a TGA. As mentioned in the paragraph 2.3.1, we performed this type of calibration also for ^{111}Cd (shown in Fig. S3 in ESI†) and used those two calibration curves to quantify the metal emissions during the evaporation experiment with the mixture of metal chlorides. In summary, as Fig. 3 is showing, not only elemental detection is performed with high resolving power but also the determination of the mass contribution of a specific element in the overall PSD is possible.

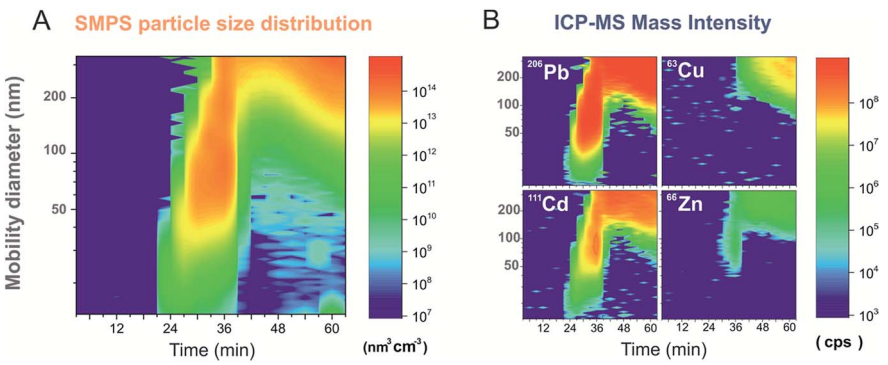

Fig. 2 (A): SMPS particle size volume distribution of the overall amount of particles generated; (B): ICP-MS intensities of ^{206}Pb, ^{63}Cu, ^{111}Cd, ^{66}Zn (same scale of intensities for all of them).

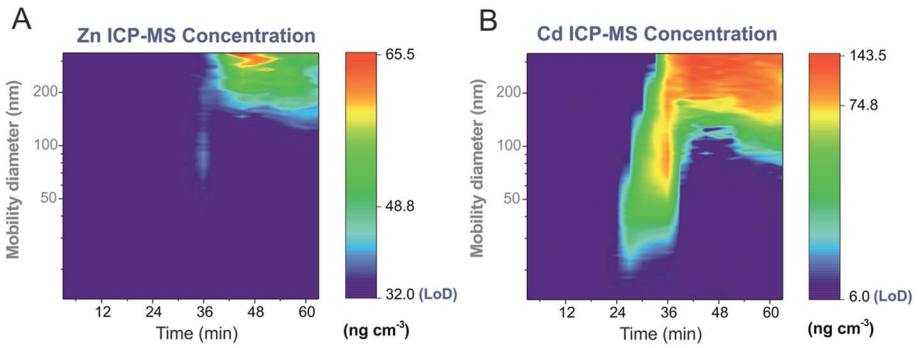

Fig. 3 Zn (A) and Cd (B) concentration obtained by extrapolation from TGA-ICP-MS calibration.

The results of this analytical method are promising and it can be applied for different applications. For instance, to study thermochemical and kinetical properties, as the evaporation rate of high boiling point metal compounds. In previous attempts by Ludwig *et al.*,[21,22] only the elemental composition was acquired, whereas the SMPS-ICP-MS setup can help to obtain size-resolved and elemental information at the same time. On the other hand, characterization of flame-synthesized particles and inorganic particles detection from diesel engines or combustion emissions might be as well interesting as other applications for the RDD-SMPS-ICP-MS system, since the concentration levels are high and often requires an extensive dilution.

3.2 ZnO nano-objects from impregnated wood combustion: Zn estimation

Wood combustion experiments were carried out to study the effect of the heterogeneous nature of a real sample, where several gas species and particulate matter (PM) are generated. In particular, we tracked the release of ZnO nanoparticles during the combustion of impregnated wood.

Wochele *et al.*[23] showed in their similarity laws that the volatilization of heavy metals can be modelled in good approximation even in a scale-down furnace, instead of using a large waste incinerator. Thus, real combustion conditions were simulated in scale-bench experiments using a tubular furnace. Although qualitative information could be extracted and the release of ZnO nano-objects was demonstrated,[20] so far it was not possible to deduce quantitative information as well. Analytical methods for the determination of metals emissions from stationary sources (such as Method 29, from the Environmental Protection Agency[24]) often include the use of quartz fibre filters for PM and impinger bottles for gaseous emissions, with following offline analysis with ICP-OES (inductively coupled plasma emission spectroscopy), ICP-MS or CV-AAS (cold vapour atomic absorption spectroscopy). Most of the studies on wood combustion emissions presented a similar approach regarding PM elemental analysis, with collection of the particles onto analytical filters and subsequent ICP-MS analysis, while the size distribution is often determined with SMPS or FMPS (fast mobility particle sizer) and ELPI (electrical low-pressure impactor) or HRLPI (high-resolution low-pressure cascade impactor). Other offline methods to assess the concentration of trace metal in aerosol samples are XRF (X-ray fluorescence) or PIXE (proton-induced X-ray emission).[25–28] Some exceptions were although including an online strategy, such as trace metal analysis on soot particles by SP-AMS[19] or organic emissions determination by SPI-ToF-AMS.[29] Those methods require anyway an extensive data treatment and availability of molecular fragmentation tables.

The quantification of Zn for combustion generated nanoparticles was here performed using the calibration strategy coupling a TGA, described before. Fig. 4 is showing on the right side the ICP-MS intensities measured as a function of the

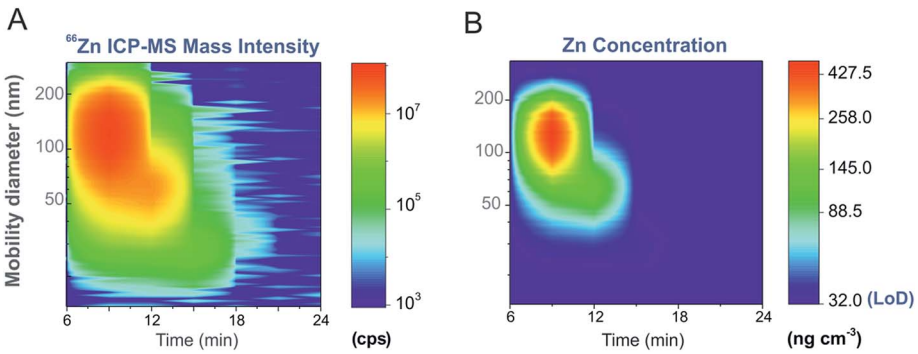

Fig. 4 ICP-MS measured intensities for ^{66}Zn ((A) adapted from Foppiano *et al.*[20] Copyright 2018 American Chemical Society) and calculated concentration of Zn (B).

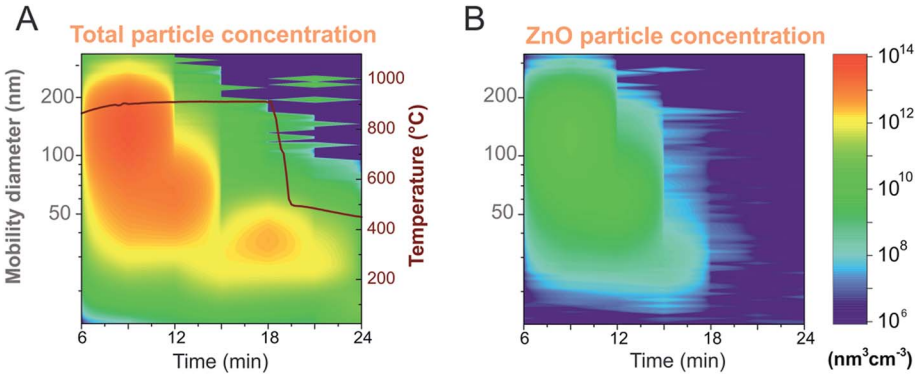

Fig. 5 Volume distribution of the total amount of particles generated ((A) adapted from Foppiano *et al.*[20] Copyright 2018 American Chemical Society) and volume distribution of ZnO only (B). The right colour scale (nm^3 cm^{-3}) is valid for both plots.

mobility diameter and time and the corresponding Zn concentration on the left side. The temperature program used for this study is shown in Fig. 5A. Most of the Zn-containing particles were emitted after the fast pyrolysis and during the combustion at 900 °C, whose concentrations lie all well beyond the LoD of the method and are represented in Fig. 4B.

A matrix-matched calibration might deliver more accurate quantification.[6] However, due to the high dilution applied no substantial matrix effects were expected. Indeed, the monitoring of the plasma stability through ^{124}Xe signal, acquired during the whole experiments, confirmed this supposition. Assuming that the entire Zn concentration hereby measured can be referred to ZnO nano-objects, this latter can be expressed also as volume-related concentration using the density of bulk ZnO (Fig. 5B). Apart from knowing the effective density would lead to more accurate results,[1] the quantification of the volume concentration of ZnO is succeeded. Moreover, possible incongruences due to geometrical factors are bypassed by gathering the ZnO volume-related PSD from the Zn concentration measured in ICP-MS. The ZnO nanoparticles presented morphology rather similar to a nano-rod than a sphere.[20] Those deviations from the spherical geometry could lead to significant changes in particle mobility diameter. The range of voltages applied and the low electric field caused in this case a random orientation of the particles, without any preferential particle alignment during the size-selection into the DMA.[30,31]

As a result of Fig. 5A and B comparison, it can be concluded that the volume concentration of ZnO can be tracked and discriminated from the total PSD even though it gives in a very small contribution. This observation is consistent with the studies of Elsasser and Leavey, who both reported how a higher ratio of organic matter is generated during each stage of wood combustion in comparison with the inorganic fraction.[32,33]

4 Conclusions

In the two parts of this study, it was shown how the external calibration of RDD-SMPS-ICP-MS with a TGA was a successful strategy to express the ICP-MS intensities as concentration. Moreover, by coupling SMPS and ICP-MS not only additional elemental information can be obtained but also a direct comparison and corrections for possible underestimations of SMPS data. Even though the organic matter released during the process exceeded consistently the inorganic fraction, it was still possible to resolve the contribution of ZnO nano-objects, track their emission with a good time-resolution and provide the Zn concentration. In this work, we proved also the resolving power of the technique in a complex matrix and for heterogeneous conditions such as during the combustion of impregnated wood.

However, especially for heterogeneous samples it is suggested that in the future a matrix-matched calibration approach would be used, which could better take into account also matrix effect. The majority of the studies on emission from stationary sources includes mainly off-line analyses with separated PSD measurement and elemental composition determination, whereas for online studies AMS related techniques are primarily reported in the literature.

The RDD-SMPS-ICP-MS system here considered is extremely useful for an initial screening of metallic particles even among complex mixtures including a size and time-resolved acquisition with a faster data treatment, needless of extensive molecular databases. The use of complementary techniques is nevertheless advisable to collect information regarding the speciation, further transformation occurring in the gas and the morphology of the particles emitted.

Conflicts of interest

There are no conflicts to declare.

Acknowledgements

Financial support by the Swiss National Science Foundation (Projects 139136 and 136890), the Swiss Nanoscience Institute (Argovia, Project NanoFil), the Energy System Integration (ESI) at PSI and the Swiss Competence Center for Energy Research SCCER BIOSWEET of the Swiss Innovation Agency Innosuisse, are gratefully acknowledged.

References

1 D. Foppiano, M. Tarik, E. Müller Gubler and C. Ludwig, *J. Anal. At. Spectrom.*, 2018, DOI: 10.1039/c8ja00066b.
2 P. Krystek, A. Ulrich, C. C. Garcia, S. Manohar and R. Ritsema, *J. Anal. At. Spectrom.*, 2011, **26**, 1701–1721.
3 R. B. Reed, C. P. Higgins, P. Westerhoff, S. Tadjiki and J. F. Ranville, *J. Anal. At. Spectrom.*, 2012, **27**, 1093.
4 I. Strenge and C. Engelhard, *J. Anal. At. Spectrom.*, 2016, **31**, 135–144.
5 S. Gschwind, L. Flamigni, J. Koch, O. Borovinskaya, S. Groh, K. Niemax and D. Günther, *J. Anal. At. Spectrom.*, 2011, **26**, 1166.
6 S. Gschwind, H. Hagendorfer, D. a. Frick and D. Gu, *Anal. Chem.*, 2013, **85**, 5875–5883.
7 O. Borovinskaya, B. Hattendorf, M. Tanner, S. Gschwind and D. Günther, *J. Anal. At. Spectrom.*, 2013, **28**, 226–233.
8 O. Borovinskaya, S. Gschwind, B. Hattendorf, M. Tanner and D. Günther, *Anal. Chem.*, 2014, **86**, 8142–8148.
9 B. Meermann and F. Laborda, *J. Anal. At. Spectrom.*, 2015, **30**, 1226–1228.
10 S. Motellier, N. Pelissier and J. G. Mattei, *J. Anal. At. Spectrom.*, 2017, **32**, 1348–1358.
11 M. Hadioui, V. Merdzan and K. J. Wilkinson, *Environ. Sci. Technol.*, 2015, **49**, 6141–6148.
12 L. Li, M. Stoiber, A. Wimmer, Z. Xu, C. Lindenblatt, B. Helmreich and M. Schuster, *Environ. Sci. Technol.*, 2016, **50**, 6327–6333.
13 D. Mozhayeva and C. Engelhard, *Anal. Chem.*, 2017, **89**, 9767–9774.
14 M. D. Montaño, J. W. Olesik, A. G. Barber, K. Challis and J. F. Ranville, *Anal. Bioanal. Chem.*, 2016, **408**, 5053–5074.
15 S. Lee, X. Bi, R. B. Reed, J. F. Ranville, P. Herckes and P. Westerhoff, *Environ. Sci. Technol.*, 2014, **48**, 10291–10300.
16 D. Salcedo, A. Laskin, V. Shutthanandan and J. L. Jimenez, *Aerosol Sci. Technol.*, 2012, **46**, 1187–1200.
17 T. Streibel, J. Schnelle-Kreis, H. Czech, H. Harndorf, G. Jakobi, J. Jokiniemi, E. Karg, J. Lintelmann, G. Matuschek, B. Michalke, L. Müller, J. Orasche, J. Passig, C. Radischat, R. Rabe, A. Reda, C. Rüger, T. Schwemer, O. Sippula, B. Stengel, M. Sklorz, T. Torvela, B. Weggler and R. Zimmermann, *Environ. Sci. Pollut. Res.*, 2016, 1–16.
18 H. Czech, O. Sippula, M. Kortelainen, J. Tissari, C. Radischat, J. Passig, T. Streibel, J. Jokiniemi and R. Zimmermann, *Fuel*, 2016, **177**, 334–342.
19 S. Carbone, T. Onasch, S. Saarikoski, H. Timonen, K. Saarnio, D. Sueper, T. Rönkkö, L. Pirjola, A. Haÿrinen, D. Worsnop and R. Hillamo, *Atmos. Meas. Tech.*, 2015, **8**, 4803–4815.
20 D. Foppiano, M. Tarik, E. Müller Gubler and C. Ludwig, *Environ. Sci. Technol.*, 2018, **52**, 895–903.
21 C. Ludwig, H. Lutz, J. Wochele and S. Stucki, *Anal. Bioanal. Chem.*, 2001, **371**, 1057–1062.
22 C. Ludwig, J. Wochele and U. Jörimann, *Anal. Chem.*, 2007, **79**, 2992–2996.
23 C. Keller, C. Ludwig, F. Davoli and J. Wochele, *Environ. Sci. Technol.*, 2005, **39**, 3359–3367.
24 Environmental Protection Agency (EPA), *Method 29-Determination of Metals Emissions from Stationary Sources*, 8/2/2017, https://www.epa.gov/emc/method-29-metals-emissions-stationary-sources.
25 A. L. Elled, L. E. Åmand and D. Eskilsson, *Energy Fuels*, 2008, **22**, 1519–1526.
26 A. Arffman, J. Yli-Ojanperä, J. Kalliokoski, J. Harra, L. Pirjola, P. Karjalainen, T. Rönkkö and J. Keskinen, *J. Aerosol Sci.*, 2014, **78**, 97–109.
27 M. Savolahti, N. Karvosenoja, J. Tissari, K. Kupiainen, O. Sippula and J. Jokiniemi, *Atmos. Environ.*, 2016, **140**, 495–505.
28 O. Sippula, H. Lamberg, J. Leskinen, J. Tissari and J. Jokiniemi, *Fuel*, 2017, **202**, 144–153.
29 H. Czech, S. M. Pieber, P. Tiitta, O. Sippula, M. Kortelainen, H. Lamberg, J. Grigonyte, T. Streibel, A. S. H. Prévot, J. Jokiniemi and R. Zimmermann, *Atmos. Environ.*, 2017, **158**, 236–245.
30 A. Zelenyuk, Y. Cai and D. Imre, *Aerosol Sci. Technol.*, 2006, **40**, 197–217.
31 A. Zelenyuk and D. Imre, *Aerosol Sci. Technol.*, 2007, **41**, 112–124.
32 A. Leavey, S. Patel, R. Martinez, D. Mitroo, C. Fortenberry, M. Walker, B. Williams and P. Biswas, *Environ. Res.*, 2017, **158**, 33–42.
33 M. Elsasser, C. Busch, J. Orasche, C. Schön, H. Hartmann, J. Schnelle-Kreis and R. Zimmermann, *Energy Fuels*, 2013, **27**, 4959–4968.

